Available online at www.sciencedirect.com

ScienceDirect

International Journal of Solids and Structures 44 (2007) 4770–4783

INTERNATIONAL JOURNAL OF SOLIDS and STRUCTURES

www.elsevier.com/locate/ijsolstr

Finite-part integral and boundary element method to solve three-dimensional crack problems in piezoelectric materials

T.Y. Qin [a,*], Y.S. Yu [a], N.A. Noda [b]

[a] College of Science, China Agricultural University, Beijing 100083, PR China
[b] Department of Mechanical Engineering, Kyushu Institute of Technology, Kitakyushu 804-8550, Japan

Received 7 April 2006; received in revised form 19 September 2006
Available online 8 December 2006

Abstract

Using the hypersingular integral equation method based on body force method, a planar crack in a three-dimensional transversely isotropic piezoelectric solid under mechanical and electrical loads is analyzed. This crack problem is reduced to solve a set of hypersingular integral equations. Compare with the crack problems in elastic isotropic materials, it is shown that for the impermeable crack, the intensity factors for piezoelectric materials can be obtained from those for elastic isotropic materials. Based on the exact analytical solution of the singular stresses and electrical displacements near the crack front, the numerical method of the hypersingular integral equation is proposed by the finite-part integral method and boundary element method, which the square root models of the displacement and electric potential discontinuities in elements near the crack front are applied. Finally, the numerical solutions of the stress and electric field intensity factors of some examples are given.

Keywords: Piezoelectric; Crack; Body force method; Boundary element method; Hypersingular integral equation

1. Introduction

The piezoelectric materials have coupled effects between the elastic and the electric fields, and have become of major interest as the functional materials such as actuators and sensors. It is possible to make a system of intelligent composite materials by combining these piezoelectric materials with structural materials. On the other hand, both electrical and mechanical disturbances are present in piezoelectric components, and the strength of the piezoelectric materials is weakened by the presence of defects such as voids and cracks. The reliability of these structures depends on the knowledge of applied mechanical and electric disturbances. When cracks are present, they may grow under service load and affect the performance of structures. Due to the disadvantage of brittleness and low fracture toughness of piezoelectric materials, a considerable number of research works have been carried out to investigate the fracture behavior (Deeg, 1980; Pak, 1990; Suo and

* Corresponding author. Fax: +86 10 62736777.
E-mail address: tyqin@cau.edu.cn (T.Y. Qin).

0020-7683/$ - see front matter © 2006 Elsevier Ltd. All rights reserved.
doi:10.1016/j.ijsolstr.2006.12.002

Kuo et al., 1992; Wang, 1992; Norris, 1994; Park and Sun, 1995; Shang et al., 2003; Kumar and Singh, 1996; Hill and Farris, 1998; McMeeking, 1999; Qin, 2001; Wang and Huang, 1995; Liu and Fan, 2001; Rajapakse and Xu, 2001; Khutoryansky and Sosa, 1995; Dunn and Wienecke, 1996; Daros and Antes, 2000; Chen and Lin, 1995; Wang and Zhang, 2005).

Because of mathematical difficulties to treat the coupled electromechanical fields in piezoelectricity, the majority of the literature concerning crack problems is based on two-dimensional assumptions. Comparatively, few exact solutions are available in the literature for three-dimensional crack problems in piezoelectric materials. Wang and Huang (1995) obtained the solution for an elliptical crack under uniform tractions and electric disturbance, if the plane of transversal isotropy is parallel to the crack. Closed-form solutions for other 3D crack configurations in an infinite piezoelectric body are yet to be found. Thus, to assess crack-like defects in piezoelectric materials under combined mechanical and electric loadings more efficiently, it is necessary to establish appropriate numerical tools. There are two important numerical methods. One is the finite element method (FEM), and another is the boundary element method (BEM). Shang et al. (2003) have analyzed penny-shaped and elliptical cracks subjected to combined mechanical tension and electric fields by FEM, and presented some numerical results of the stress intensity factors and energy release rates. BEM is a powerful tool for the solution of field problems of mathematical physics, since it offers some inherent advantages over FEM, like the discretization of the boundary only and an improved accuracy in flux calculations. Many publications have already been devoted to the development of fundamental solutions and BEM for piezoelectricity (Deeg, 1980, 2001,), but only a very limited number of them deals with three-dimensional analyses, due to the problems involved resulting from the anisotropy of piezoelectric materials. A 3D Green's function for static piezoelectricity and its derivatives have been presented by Deeg (1980) for piezoelectrics of general anisotropy. Dynamic piezoelectric Green's functions have been presented by Norris (1994) in the frequency domain and by Khutoryansky and Sosa (1995) in the time domain. For the particular case of transversely isotropic piezoelectricity, Dunn and Wienecke (1996) for piezoelectrostatics, and Daros and Antes (2000) for transient analysis developed simplified expressions for the Green's functions. BEM for static piezoelectricity with corresponding numerical results for 3D analysis has been presented by Chen and Lin (1995), and by Hill and Farris (1998). Wang and Zhang (2005) have applied the electrical field saturation model to the fracture prediction of piezoelectric materials containing electrically impermeable cracks, and obtained the stress intensity factor and the energy release rate in closed-form. Zhao and Shen et al. (1997) has investigated the crack problems in piezoelectric materials by BEM and hypersingular integral equation, and given a solution for circular crack. A set hypersingular integral equations and some numerical results for a planar crack in an infinite transversely isotropic piezoelectric media has been given by Chen (2003), in which the unknown function is approximated with a product of the fundamental density function and polynomials. Qin and Noda (2004) have derived a set of hypersingular integral equations of a three-dimensional crack problem in piezoelectric materials, and obtained the exact analytical solutions of the singular stresses and electrical displacements near the crack front in a transversely isotropic piezoelectric solid, but not given the numerical method and solutions.

In this paper, based on the exact analytical solution of the singular stresses and electrical displacements near the crack front, a numerical method for the crack problems in a three-dimensional transversely isotropic piezoelectric solid was proposed by the finite-part integral method and boundary element method. It is shown that for impermeable cracks, the numerical values of the dimensionless intensity factors of K_{I} and K_{IV} are equal to that of the dimensionless intensity factor of mode I for elastic isotropic materials.

2. Basic of piezoelectricity

The linear governing equations and constitutive relations for a piezoelectric material in static equilibrium can be expressed as two separate equations, one representing conservation of momentum and the other conservation of electric charge (Deeg, 1980; Pak, 1990; Suo and Kuo et al., 1992; Wang, 1992). To use these two equations in conjunction with the developed boundary integral equation method, they are combined into one. In these equations, lowercase indices i,l can have values of 1, 2, or 3, and uppercase indices I can take on values of 1, 2, 3, and 4. The modified governing equation for the piezoelectric material in static equilibrium can be written as (Deeg, 1980)

$$\Sigma_{iJ,i} + b_J = 0 \tag{1}$$

where Σ_{iJ} is the stress-electric displacement matrix, defined as

$$\Sigma_{iJ} = \begin{cases} \sigma_{ij} & \text{for} \quad J = j = 1,2,3 \\ D_i & \text{for} \quad J = 4 \end{cases} \tag{2}$$

and b_J is the body load (force and charge) column vector. A subscript comma denotes the partial differentiation. The combined constitutive equation is written as

$$\Sigma_{iJ} = E_{iJKl} Z_{Kl} \tag{3}$$

where E_{iJKl} is the electroelastic constant matrix

$$E_{iJKl} = \begin{cases} c_{ijkl} & \text{for} \quad J,K = 1,2,3 \\ e_{lij} & \text{for} \quad J = 1,2,3, \quad K = 4 \\ e_{ikl} & \text{for} \quad J = 4, \quad K = 1,2,3, \\ -a_{il} & \text{for} \quad J = 4, \quad K = 4 \end{cases} \tag{4}$$

and the strain-electric field matrix Z_{Kl} takes the form

$$Z_{Kl} = \begin{cases} \varepsilon_{kl} & \text{for} \quad K = k = 1,2,3 \\ \phi_{,l} & \text{for} \quad K = 4 \end{cases} \tag{5}$$

In addition, U_K is the elastic displacement-electric potential matrix

$$U_K = \begin{cases} u_k & \text{for} \quad K = k = 1,2,3 \\ \phi & \text{for} \quad K = 4 \end{cases} \tag{6}$$

where u_k and ϕ are the elastic displacement and electric potential, respectively.

3. General solutions for a crack in piezoelectric materials

3.1. Boundary condition of a crack surface

The mechanical boundary condition of cracks in piezoelectric materials is always defined by stress-free crack surfaces. Several electric boundary conditions were proposed in literature. Among these electric boundary conditions, two different conditions are applied widely. Those are permeable and impermeable conditions. For the first one, the electric potential and the normal electric displacement should be continuous across the crack surface

$$D_3^+ = D_3^- \quad \phi^+ = \phi^- \tag{7}$$

where the superscripts + and − denote the upper and lower crack surfaces, respectively. This aspect has been supported by McMeeking (1999), and Dunn and Wienecke (1996). Pak (1990), and Suo and Kuo et al. (1992) proposed impermeable conditions on the crack faces

$$D_3^+ = D_3^- = 0 \tag{8}$$

This paper presents an analysis for the crack problems in piezoelectric materials based on boundary condition (8).

3.2. General solutions for a crack in a three-dimensional infinite piezoelectric solid

Consider a flat crack S in an infinite three-dimensional piezoelectric solid. A fixed rectangular Cartesian system x_i ($i = 1,2,3$) is used. The crack is assumed to be in the x_1x_2 plane, and normal to the x_3 axis. Using the fundamental solution of the piezoelectric material, the elastic displacements and the electric potential at an interior point p can be expressed as (Qin and Noda, 2004)

$$U_I(p) = -\int_{S^+} T^+_{IJ}(p,Q)\tilde{U}_J(Q)\mathrm{d}s(Q), \qquad I,J = 1,2,3,4 \tag{9}$$

where Q (or Q^+) is a point on the upper crack surface S^+, and $T^+_{IJ}(p,Q) = T_{IJ}(p,Q^+) = -T^{(}_{IJ}p,Q^-)$ is the value of the fundamental solutions of the piezoelectric material T_{IJ} at upper crack surface S^+, which is related the Green's function as follows (Hill and Farris, 1998)

$$T_{IJ}(p,Q) = E_{kJMn}\frac{\partial G_{IM}(p,Q)}{\partial \xi_n}n_k \tag{10}$$

where n_k is the unit outward normal vector, ξ_n is the coordinate of point Q, $\tilde{U}_J$ is the elastic displacement or electric potential discontinuity, and can be written as

$$\tilde{U}_J = \begin{cases} \tilde{u}_j = u_j^+ - u_j^- & \text{for} \quad J = j = 1,2,3 \\ \tilde{\phi} = \phi^+ - \phi^- & \text{for} \quad J = 4 \end{cases} \tag{11}$$

Using solution (9) and constitutive Eq. (3), the corresponding stress and electric displacements are expressed as

$$\Sigma_{iJ}(p) = -\int_{S^+} S^+_{KiJ}(p,Q)\tilde{U}_K(Q)\mathrm{d}s(Q) \tag{12}$$

where the integral kernel is as follows

$$S_{KiJ}(p,Q) = E_{iJMn}\frac{\partial T_{MK}(p,Q)}{\partial x_n} = -E_{iJMn}\frac{\partial T_{MK}(p,Q)}{\partial \xi_n} \tag{13}$$

3.3. Green's solution

For the transversely isotropic piezoelectric material, the electro-elastic constants can be written as follows:

$$\begin{aligned} c_{ijkl} &= c_{12}\delta_{ij}\delta_{kl} + c_{66}(\delta_{ik}\delta_{jl} + \delta_{il}\delta_{jk}) + (c_{13} - c_{12})(\delta_{ij}\delta_{3k}\delta_{3l} + \delta_{3i}\delta_{3j}\delta_{kl}) \\ &\quad + (c_{44} - c_{66})(\delta_{jk}\delta_{3i}\delta_{3l} + \delta_{ik}\delta_{3j}\delta_{3l} + \delta_{il}\delta_{3j}\delta_{3k} + \delta_{jl}\delta_{3i}\delta_{3k}) \\ &\quad + (c_{11} + c_{33} - 2c_{13} - 4c_{44})\delta_{3i}\delta_{3j}\delta_{3k}\delta_{3l} \end{aligned} \tag{14}$$

$$e_{lij} = e_{31}\delta_{ij}\delta_{3l} + e_{15}(\delta_{il}\delta_{3j} + \delta_{jl}\delta_{3i}) + (e_{33} - c_{31} - 2e_{15})\delta_{3i}\delta_{3j}\delta_{3l} \tag{15}$$

$$a_{il} = a_{11}\delta_{il} + (a_{33} - a_{a1})\delta_{3i}\delta_{3l} \tag{16}$$

here $c_{66} = (c_{11} - c_{12})/2$. For transversely isotropic piezoelectric, Green's function can be written as an explicit expression. Here we use the solutions given by Dunn and Wienecke (1996) by a potential method. The governing equations are expressed as

$$\begin{cases} u_1 = \left\{(c_{13}e_{15} - c_{44}e_{31})\frac{\partial^2}{\partial x_1\partial x_3}\left(\frac{\partial^2}{\partial x_1^2} + \frac{\partial^2}{\partial x_2^2}\right) + [(c_{44} + c_{13})e_{33} - c_{33}(e_{15} + e_{31})]\frac{\partial^4}{\partial x_1\partial x_3^3}\right\}g - \frac{\partial\psi}{\partial x_2} \\ u_2 = \left\{(c_{13}e_{15} - c_{44}e_{31})\frac{\partial^2}{\partial x_2\partial x_3}\left(\frac{\partial^2}{\partial x_1^2} + \frac{\partial^2}{\partial x_2^2}\right) + [(c_{44} + c_{13})e_{33} - c_{33}(e_{15} + e_{31})]\frac{\partial^4}{\partial x_2\partial x_3^3}\right\}g + \frac{\partial\psi}{\partial x_1} \\ u_3 = \left\{-c_{11}e_{15}\left(\frac{\partial^2}{\partial x_1^2} + \frac{\partial^2}{\partial x_2^2}\right)^2 - c_{44}e_{33}\frac{\partial^4}{\partial x_3^4} + [c_{13}(e_{15} + e_{31}) + c_{44}e_{31} - c_{11}e_{33}]\frac{\partial^2}{\partial x_3^2}\left(\frac{\partial^2}{\partial x_1^2} + \frac{\partial^2}{\partial x_2^2}\right)\right\}g \\ \phi = [c_{44}c_{11}\left(\frac{\partial^2}{\partial x_1^2} + \frac{\partial^2}{\partial x_2^2}\right)^2 + c_{44}c_{33}\frac{\partial^4}{\partial x_3^4} + (c_{11}c_{33} - 2c_{44}c_{13} - c_{13}^2)\frac{\partial^2}{\partial x_3^2}\left(\frac{\partial^2}{\partial x_1^2} + \frac{\partial^2}{\partial x_2^2}\right)\Big\}g \end{cases} \tag{17}$$

where the potentials g and ψ must satisfy following equations:

$$\left(\frac{\partial^2}{\partial x_1^2}+\frac{\partial^2}{\partial x_2^2}+\frac{1}{v_1^2}\frac{\partial^2}{\partial x_3^2}\right)\left(\frac{\partial^2}{\partial x_1^2}+\frac{\partial^2}{\partial x_2^2}+\frac{1}{v_2^2}\frac{\partial^2}{\partial x_3^2}\right)\left(\frac{\partial^2}{\partial x_1^2}+\frac{\partial^2}{\partial x_2^2}+\frac{1}{v_3^2}\frac{\partial^2}{\partial x_3^2}\right)g=0 \tag{18}$$

$$\left(\frac{\partial^2}{\partial x_1^2}+\frac{\partial^2}{\partial x_2^2}+\frac{1}{v_0^2}\frac{\partial^2}{\partial x_3^2}\right)\psi=0 \tag{19}$$

here $v_0=\sqrt{c_{66}/c_{44}}$, and $-1/v_1^2$, $-1/v_2^2$, $-1/v_3^2$ are the roots of the following cubic equation:

$$s^3+\frac{a}{d}s^2+\frac{b}{d}s+\frac{c}{d}=0 \tag{20}$$

where

$$\begin{cases} a=c_{11}(a_{11}c_{33}+2e_{15}e_{33})-a_{11}c_{13}(c_{13}+2c_{44})+c_{44}(a_{33}c_{11}+e_{31}^2)-2e_{15}c_{13}(e_{31}+e_{15}) \\ b=c_{33}[a_{11}c_{44}+a_{33}c_{11}+e_{31}(e_{31}+e_{15})]-c_{13}a_{33}(c_{13}+2c_{44})+(e_{15}+e_{31})(c_{33}e_{15}-2c_{13}e_{33}) \\ \qquad +e_{33}(c_{11}e_{33}-2c_{44}e_{31}) \\ c=c_{44}(a_{33}c_{33}+e_{33}^2) \\ d=c_{11}(a_{11}c_{44}+e_{15}^2) \end{cases} \tag{21}$$

If the above Eqs. (18) and (19) are solved for a point charge or force, the Green's functions can be obtained from the solutions u_i and ϕ.

3.3.1. Point force charge

For a unit point charge at point $\boldsymbol{\xi}(\xi_1,\xi_2,\xi_3)$, the elastic displacements and electric potential at point $\boldsymbol{x}(x_1,x_2,x_3)$ can be expressed as

$$\begin{cases} u_1=\sum_{i=1}^{3}A_i\lambda_i^u\frac{x_1-\xi_1}{R_iR_i^*}, \quad u_2=\sum_{i=1}^{3}A_i\lambda_i^u\frac{x_2-\xi_2}{R_iR_i^*} \\ u_3=\sum_{i=1}^{3}A_i\lambda_i^w\frac{1}{R_i}, \qquad \phi=\sum_{i=1}^{3}A_i\lambda_i^\phi\frac{1}{R_i} \end{cases} \tag{22}$$

where

$$\begin{cases} R_i=\sqrt{(x_1-\xi_1)^2+(x_2-\xi_2)^2+z_i^2} \\ R_i^*=R_i+z_i, \qquad\qquad i=0,1,2,3 \\ z_i=v_i(x_3-\xi_3) \end{cases} \tag{23}$$

$$\begin{cases} \lambda_i^u=[(c_{13}+c_{44})e_{33}-c_{33}(e_{15}+e_{31})]v_i^3+(c_{44}e_{31}-c_{13}e_{15})v_i \\ \lambda_i^w=-c_{44}e_{33}v_i^4-[e_{31}(c_{13}+c_{44})-e_{33}c_{11}+e_{15}c_{13}]v_i^2-c_{11}e_{15} \\ \lambda_i^\phi=c_{33}c_{44}v_i^4+[c_{13}(c_{13}+2c_{44})-c_{11}c_{33}]v_i^2+c_{44}c_{11} \end{cases} \tag{24}$$

and A_i is determined by following equations:

$$\sum_{i=1}^{3}A_i\lambda_i^u=0 \quad \sum_{i=1}^{3}A_i\frac{n_i^a}{v_i^2-1}=0 \quad \sum_{i=1}^{3}A_i\frac{n_i^e}{v_i^2-1}=\frac{1}{2\pi} \tag{25}$$

here

$$\begin{cases} n_i^a=2\left[\lambda_i^u(c_{13}+c_{44}v_i^2)+v_i\lambda_i^w(c_{44}-c_{33})+v_i\lambda_i^\phi(e_{15}-e_{33})\right] \\ n_i^e=2\left[-\lambda_i^u(e_{31}+e_{15}v_i^2)+v_i\lambda_i^w(e_{33}-e_{15})+v_i\lambda_i^\phi(a_{11}-a_{33})\right] \end{cases} \tag{26}$$

3.3.2. Point force in x_3-direction

For a unit point force in x_3-direction at point $\boldsymbol{\xi}(\xi_1,\xi_2,\xi_3)$, the elastic displacements and electric potential at point $\boldsymbol{x}(x_1,x_2,x_3)$ is expressed as

$$\begin{cases} u_1 = \sum_{i=1}^{3} B_i \lambda_i^u \frac{x_1-\xi_1}{R_i R_i^*}, \quad u_2 = \sum_{i=1}^{3} B_i \lambda_i^u \frac{x_2-\xi_2}{R_i R_i^*} \\ u_3 = \sum_{i=1}^{3} B_i \lambda_i^w \frac{1}{R_i}, \qquad \phi = \sum_{i=1}^{3} B_i \lambda_i^\phi \frac{1}{R_i} \end{cases} \tag{27}$$

where B_i satisfies following equations

$$\sum_{i=1}^{3} B_i \lambda_i^u = 0, \quad \sum_{i=1}^{3} B_i \frac{n_i^a}{v_i^2 - 1} = \frac{1}{2\pi} \quad \sum_{i=1}^{3} B_i \frac{n_i^e}{v_i^2 - 1} = 0 \tag{28}$$

3.3.3. Point force in x_1-direction

For a unit point force in x_1-direction at point $\boldsymbol{\xi}(\xi_1,\xi_2,\xi_3)$, the elastic displacements and electric potential at point $\boldsymbol{x}(x_1,x_2,x_3)$ is expressed as

$$\begin{cases} u_1 = D_0 \left[\frac{1}{R_0} - \frac{(x_2-\xi_2)^2}{R_0 R_0^{*2}} \right] - \sum_{i=1}^{3} D_i \lambda_i^u \left[\frac{1}{R_i^*} - \frac{(x_1-\xi_1)^2}{R_i R_i^{*2}} \right] \\ u_2 = (x_1 - \xi_1)(x_2 - \xi_2) \left(D_0 \frac{1}{R_0 R_0^{*2}} + \sum_{i=1}^{3} D_i \lambda_i^u \frac{1}{R_i R_i^{*2}} \right) \\ u_3 = \sum_{i=1}^{3} D_i \lambda_i^w \frac{(x_1-\xi_1)}{R_i R_i^*} \\ \phi = \sum_{i=1}^{3} D_i \lambda_i^\phi \frac{(x_1-\xi_1)}{R_i R_i^*} \end{cases} \tag{29}$$

where D_i satisfies

$$\begin{cases} D_0 v_0 + \sum_{i=1}^{3} D_i v_i \lambda_i^u = 0, \quad \sum_{i=1}^{3} D_i \lambda_i^w = 0 \\ \sum_{i=1}^{3} D_i \lambda_i^\phi = 0, \qquad D_0 v_0 c_{44} + \sum_{i=1}^{3} D_i \frac{n_i^t}{v_i^2-1} = \frac{1}{2\pi} \end{cases} \tag{30}$$

here

$$n_i^t = v_i \lambda_i^u (c_{44} - c_{11}) + \lambda_i^w (c_{44} + c_{13} v_i^2) + \lambda_i^\phi (e_{15} + e_{31} v_i^2) \tag{31}$$

4. Hypersingular integral equations

Using the boundary conditions, the hypersingular integral equations for a flat crack in an infinite transversely isotropic piezoelectric solid can be obtained. Let the source point p be taken to the upper crack surface and represented by P, using the elastic and electric boundary conditions of the crack surface, the hypersingular integral equations can be obtained as (Qin and Noda, 2004)

$$= \!\!\!\!\!\!\!\!\int_{S^+} \frac{1}{r^3} [c_{44}^2 D_0 v_0^2 (2\delta_{\alpha\beta} - 3r_{,\alpha} r_{,\beta}) + k_{11}(\delta_{\alpha\beta} - 3r_{,\alpha} r_{,\beta})] \tilde{u}_\beta(Q) \mathrm{d}s(Q) = -p_\alpha(P) \ \alpha,\beta = 1,2; P \in S^+ \tag{32}$$

$$= \!\!\!\!\!\!\!\!\int_{S^+} \frac{1}{r^3} [k_{33} \tilde{u}_3(Q) + k_{34} \tilde{\phi}(Q)] \mathrm{d}s(Q) = -p_3(P) \quad P \in S^+ \tag{33}$$

$$= \!\!\!\!\!\!\!\!\int_{S^+} \frac{1}{r^3} [k_{43} \tilde{u}_3(Q) + k_{44} \tilde{\phi}(Q)] \mathrm{d}s(Q) = -q_0(P) \quad P \in S^+ \tag{34}$$

where $= \!\!\!\!\!\!\int$ means that the integral must be interpreted as a finite-part integral, and $p_i(P)$ and $q_0(P)$ represent the mechanical and electrical loads on the crack surface due to internal or external loads, and k_{IJ} is determined as

$$\begin{cases} k_{11} = \sum_{i=1}^{3}[c_{44}(B_i + D_i v_i) + e_{15}A_i][c_{44}(v_i\lambda_i^u + \lambda_i^w) + e_{15}\lambda_i^\phi] \\ k_{33} = \sum_{i=1}^{3}(e_{33}A_i v_i + c_{33}B_i v_i - c_{13}D_i)(-c_{13}\lambda_i^u + c_{33}v_i\lambda_i^w + e_{33}v_i\lambda_i^\phi) \\ k_{34} = \sum_{i=1}^{3}(-a_{33}A_i v_i + e_{33}B_i v_i - e_{31}D_i)(-c_{13}\lambda_i^u + c_{33}v_i\lambda_i^w + e_{33}v_i\lambda_i^\phi) \\ k_{43} = \sum_{i=1}^{3}(e_{33}A_i v_i + c_{33}B_i v_i - c_{13}D_i)(-e_{31}\lambda_i^u + e_{33}v_i\lambda_i^w - a_{33}v_i\lambda_i^\phi) \\ k_{44} = \sum_{i=1}^{3}(-a_{33}A_i v_i + e_{33}B_i v_i - e_{31}D_i)(-e_{31}\lambda_i^u + e_{33}v_i\lambda_i^w - a_{33}v_i\lambda_i^\phi) \end{cases} \tag{35}$$

Notice that Eq. (32) is not coupled with Eqs. (33) and (34), and can be solved independently. It means that shear modes are independent of mode I and electric mode. Eqs. (32)–(34) are hypersingular integral equations, and can be numerically solved. Solving these equations, all the unknowns can be obtained. Then the mechanical stress intensity factors corresponding to the crack modes I, II and III as well as the "electric field intensity factor" K_{IV} are defined as

$$\begin{cases} K_I = \lim_{r\to 0}\sigma_{33}(r,\theta)_{|\theta=0}\sqrt{2r}, \quad K_{II} = \lim_{r\to 0}\sigma_{32}(r,\theta)_{|\theta=0}\sqrt{2r}, \\ K_{III} = \lim_{r\to 0}\sigma_{31}(r,\theta)_{|\theta=0}\sqrt{2r} \quad K_{IV} = \lim_{r\to 0}D_3(r,\theta)_{|\theta=0}\sqrt{2r} \end{cases} \tag{36}$$

where r is the distance from point p, to the crack front point Q_0, where $(3,n,\tau)$ are the local coordinates.

5. Numerical technique

Eqs. (32)–(34) are hypersingular integral equations, and can be numerically solved by use of the boundary element method combined with the finite-part integral method (Qin and Tang, 1993, 1997). Assuming that the crack surface S^+ is divided into a number of quadrangular or triangular elements, Eqs. (32)–(34) can be reduced to a set of linear algebraic equations:

$$\sum_{m=1}^{M} a_{\alpha\beta mn}(P_n, Q_m)\tilde{u}_\beta(Q_m) = -p_\alpha(P_n) \quad \alpha,\beta = 1,2;\ n = 1,\ldots,M \quad P_n, Q_m \in S^+ \tag{37}$$

$$\sum_{m=1}^{M} c_{1mn}(P_n, Q_m)\tilde{u}_3(Q_m) + \sum_{m=1}^{M} c_{2mn}(P_n, Q_m)\tilde{\phi}(Q_m) = -p_3(P_n) \tag{38}$$

$$\sum_{m=1}^{M} d_{1mn}(P_n, Q_m)\tilde{u}_3(Q_m) + \sum_{m=1}^{M} d_{2mn}(P_n, Q_m)\tilde{\phi}(Q_m) = -q_0(P_n) \tag{39}$$

where M is the number of the total nodal points located on the surface S^+, P_n and Q_m are the nodal points, $a_{\alpha\beta mn}$, c_{1mn}, c_{2mn}, d_{1mn} and d_{2mn} are the components of coefficient matrix which can be determined by summing all the following integrals relating the reference nodal point P_n with all the elements in S^+

$$I_m = \int_{S_m} \frac{1}{r^3}[c_{44}^2 D_0 v_0^2(2\delta_{\alpha\beta} - 3r_{,\alpha}r_{,\beta}) + k_{11}(\delta_{\alpha\beta} - 3r_{,\alpha}r_{,\beta})]\tilde{u}_\beta \mathrm{d}\xi_1\,\mathrm{d}\xi_2 \quad \alpha,\beta = 1,2 \tag{40}$$

$$I'_m = \int_{S_m} \frac{1}{r^3}\tilde{u}_3 \mathrm{d}\xi_1\,\mathrm{d}\xi_2 \quad I''_m = \int_{S_m} \frac{1}{r^3}\tilde{\phi}\mathrm{d}\xi_1\,\mathrm{d}\xi_2 \tag{41}$$

Now the main task is to numerically calculate these integrals. Notice that integrals I'_m and I''_m are similar to integral I_m, and can be evaluated similarly. To improve the numerical solution precision, the elements of S^+ are divided into two groups. One is the crack front element group which is joined with the crack front, and the other is the internal element group. The integrals over the latter elements can be calculated as paper (Qin and Tang, 1993). Here the integrals over the crack front elements will be treated as follows. Among these integrals, there are not only general integrals, but also hypersingular integrals. If the reference point is not in the integrating element, the integrals are normal. For a quadrangular element, $\tilde{u}_i$ is assumed as follows

$$\tilde{u}_i = \sqrt{\frac{1-\xi}{2}}\left[\tfrac{1}{4}(1-\xi)(1-\eta)\tilde{u}_i^{(d)} + \tfrac{1}{4}(1-\xi)(1+\eta)\tilde{u}_i^{(c)} + \tfrac{1}{4}(1+\xi)(1-\eta)c_i^{(a)} + \tfrac{1}{4}(1+\xi)(1+\eta)c_i^{(b)}\right] \tag{42}$$

where (ξ,η) are the local dimensionless coordinates, $c_i^{(a)}$ and $c_i^{(b)}$ are unknown constants related to the crack front point a and b, respectively. The relative integrals can be calculated as normal one. It is noticed that $\tilde{u}_i$ defined by (42) has the $\sqrt{r}$ behavior near the crack front, which is consistent with the analytical theory (Qin and Noda, 2004). If the reference point coincides with one of the nodes of the integrating element, the integrals are hypersingular, which can be written as follows. Firstly, it is assumed that the reference point P_n coincides with internal point d. Linking point d with b, the quadrangular element is divided into two triangular elements S_{m1} and S_{m2} as shown in Fig. 1. The displacement discontinuities can be expressed as

$$\tilde{u}_i = \sqrt{(1-\frac{r}{R})}\left[L_d\tilde{u}_i^{(d)} + L_a c_i^{(a)} + L_b c_i^{(b)}\right] \quad Q \in S_{m1} \tag{43}$$

$$\tilde{u}_i = \sqrt{\left[1-(1-S_c)\frac{r}{R}\right]}\left[L_d\tilde{u}_i^{(d)} + L_c\tilde{u}_i^{(c)} + L_b c_i^{(b)}\right] \quad Q \in S_{m2} \tag{44}$$

where L_a, L_b, L_c, and L_d are the area coordinates of S_{m1} and S_{m2}, respectively, S_c is the area coordinate of point w, and R is the distance between point d and point w.

The hypersingular integrals related to (43) can be written as

$$\begin{aligned} I_{dd} &= \neq\!\!\!\!\!\!\int_{S_{m1}} \frac{1}{r^3}\left[c_{44}^2 D_0 v_0^2(2\delta_{\alpha\beta} - 3r_{,\alpha}r_{,\beta}) + k_{11}(\delta_{\alpha\beta} - 3r_{,\alpha}r_{,\beta})\right]\sqrt{1-\frac{r}{R}}L_d \mathrm{d}\xi_1\mathrm{d}\xi_2 \\ &= \neq\!\!\!\!\!\!\int_{S_{m1}} \frac{1}{r^3}\left[(c_{44}^2 D_0 v_0^2(2\delta_{\alpha\beta} - 3r_{,\alpha}r_{,\beta}) + k_{11}(\delta_{\alpha\beta} - 3r_{,\alpha}r_{,\beta})\right]\sqrt{1-\frac{r}{R}}(1-\frac{r}{R})\mathrm{d}\xi_1\mathrm{d}\xi_2 \\ &= 3\Delta(1-2\ln 2)\int_0^1 \frac{1}{R^3(\theta)}\left[c_{44}^2 D_0 v_0^2(2\delta_{\alpha\beta} - 3R_{,\alpha}R_{,\beta}) + k_{11}(\delta_{\alpha\beta} - 3R_{,\alpha}R_{,\beta})\right]\mathrm{d}S_b \end{aligned} \tag{45}$$

$$\begin{aligned} I_{da} &= \int_{S_{m1}} \frac{1}{r^3}\left[c_{44}^2 D_0 v_0^2(2\delta_{\alpha\beta} - 3r_{,\alpha}r_{,\beta}) + k_{11}(\delta_{\alpha\beta} - 3r_{,\alpha}r_{,\beta})\right]\sqrt{1-\frac{r}{R}}L_a \mathrm{d}\xi_1\mathrm{d}\xi_2 \\ &= \int_{S_{m1}} \frac{1}{r^3}\left[c_{44}^2 D_0 v_0^2(2\delta_{\alpha\beta} - 3r_{,\alpha}r_{,\beta}) + k_{11}(\delta_{\alpha\beta} - 3r_{,\alpha}r_{,\beta})\right]\sqrt{1-\frac{r}{R}}(1-S_b)\frac{r}{R}\mathrm{d}\xi_1\mathrm{d}\xi_2 \\ &= -4\Delta(1-\ln 2)\int_0^1 \frac{1}{R^3(\theta)}\left[c_{44}^2 D_0 v_0^2(2\delta_{\alpha\beta} - 3R_{,\alpha}R_{,\beta}) + k_{11}(\delta_{\alpha\beta} - 3R_{,\alpha}R_{,\beta})\right](1-S_b)\mathrm{d}S_b \end{aligned} \tag{46}$$

$$\begin{aligned} I_{db} &= -\!\!\!\!\!\!\int_{S_{m1}} \frac{1}{r^3}\left[c_{44}^2 D_0 v_0^2(2\delta_{\alpha\beta} - 3r_{,\alpha}r_{,\beta}) + k_{11}(\delta_{\alpha\beta} - 3r_{,\alpha}r_{,\beta})\right]\sqrt{1-\frac{r}{R}}L_b \mathrm{d}\xi_1\mathrm{d}\xi_2 \\ &= -\!\!\!\!\!\!\int_{S_{m1}} \frac{1}{r^3}\left[c_{44}^2 D_0 v_0^2(2\delta_{\alpha\beta} - 3r_{,\alpha}r_{,\beta}) + k_{11}(\delta_{\alpha\beta} - 3r_{,\alpha}r_{,\beta})\right]\sqrt{1-\frac{r}{R}}S_b\frac{r}{R}\mathrm{d}\xi_1\mathrm{d}\xi_2 \\ &= -4\Delta(1-\ln 2)\int_0^1 \frac{1}{R^3(\theta)}\left[c_{44}^2 D_0 v_0^2(2\delta_{\alpha\beta} - 3R_{,\alpha}R_{,\beta}) + k_{11}(\delta_{\alpha\beta} - 3R_{,\alpha}R_{,\beta})\right]S_b\mathrm{d}S_b \end{aligned} \tag{47}$$

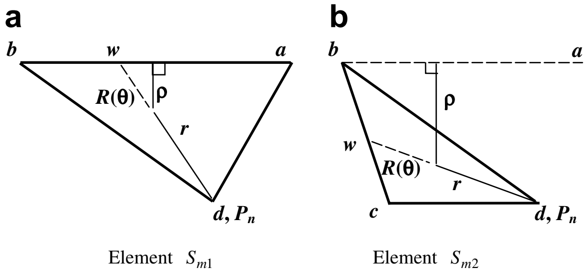

Fig. 1. A crack front element.

where Δ is the area of element S_{m1},$⨍$ is the symbol of principal-value integral, and S_b is the area coordinate of point w on the side ab. The hypersingular integrals related to (44) can be analogously treated, here only give the computing formula for the first one

$$\begin{aligned}
I_{dd} &= ⨎_{S_{m2}} \frac{1}{r^3}\left[c_{44}^2 D_0 v_0^2(2\delta_{\alpha\beta} - 3r_{,\alpha}r_{,\beta}) + k_{11}(\delta_{\alpha\beta} - 3r_{,\alpha}r_{,\beta})\right]\sqrt{1-(1-S_c)\frac{r}{R}}L_d \mathrm{d}\xi_1\,\mathrm{d}\xi_2 \\
&= 2\Delta\int_0^1 \frac{1}{R^3(\theta)}\{\left[c_{44}^2 D_0 v_0^2(2\delta_{\alpha\beta} - 3R_{,\alpha}R_{,\beta}) + k_{11}(\delta_{\alpha\beta} - 3R_{,\alpha}R_{,\beta})\right][\frac{1}{2}(3+S_c) - 3\sqrt{S_c} + (3-S_c) \\
&\quad \times \ln\left[\frac{1}{2}(1+\sqrt{S_c})\right]\}\mathrm{d}S_c
\end{aligned} \tag{48}$$

Secondly, if the reference point P_n infinitely tends to crack front point a, link point a with c, and the element is divided into two triangular elements S_{m1} and S_{m2} as shown in Fig. 2. The displacement discontinuities can be expressed as

$$\tilde{u}_i = \sqrt{\frac{r}{R}S_c}\left[L_c\tilde{u}_i^{(d)} + L_a c_i^{(a)} + L_b c_i^{(b)}\right] \quad Q \in S_{m1} \tag{49}$$

$$\tilde{u}_i = \sqrt{\frac{r}{R}}\left[L_c\tilde{u}_i^{(c)} + L_d\tilde{u}_i^{(d)} + L_a c_i^{(a)}\right] \quad Q \in S_{m2} \tag{50}$$

The hypersingular integrals related to (49) can be written as

$$\begin{aligned}
I_{aa} &= ⨎_{S_{m1}} \frac{1}{r^3}\left[c_{44}^2 D_0 v_0^2(2\delta_{\alpha\beta} - 3r_{,\alpha}r_{,\beta}) + k_{11}(\delta_{\alpha\beta} - 3r_{,\alpha}r_{,\beta})\right]\sqrt{\frac{r}{R}S_c}L_a \mathrm{d}\xi_1\,\mathrm{d}\xi_2 \\
&= \int_\alpha \left[c_{44}^2 D_0 v_0^2(2\delta_{\alpha\beta} - 3r_{,\alpha}r_{,\beta}) + k_{11}(\delta_{\alpha\beta} - 3r_{,\alpha}r_{,\beta})\right]\sqrt{S_c}\mathrm{d}\theta ⨎_0^{R(\theta)} \frac{1}{r^2}\sqrt{\frac{r}{R}}(1-\frac{r}{R})\mathrm{d}r \\
&= -8\Delta\int_0^1 \frac{1}{R^3(\theta)}\left[c_{44}^2 D_0 v_0^2(2\delta_{\alpha\beta} - 3R_{,\alpha}R_{,\beta}) + k_{11}(\delta_{\alpha\beta} - 3R_{,\alpha}R_{,\beta})\right]\sqrt{S_c}\mathrm{d}S_c
\end{aligned} \tag{51}$$

$$\begin{aligned}
I_{ab} &= ⨍_{S_{m1}} \frac{1}{r^3}\left[c_{44}^2 D_0 v_0^2(2\delta_{\alpha\beta} - 3r_{,\alpha}r_{,\beta}) + k_{11}(\delta_{\alpha\beta} - 3r_{,\alpha}r_{,\beta})\right]\sqrt{\frac{r}{R}S_c}L_b \mathrm{d}\xi_1\,\mathrm{d}\xi_2 \\
&= 4\Delta\int_0^1 \frac{1}{R^3(\theta)}\left[c_{44}^2 D_0 v_0^2(2\delta_{\alpha\beta} - 3R_{,\alpha}R_{,\beta}) + k_{11}(\delta_{\alpha\beta} - 3R_{,\alpha}R_{,\beta})\right]\sqrt{S_c}(1-S_c)\mathrm{d}S_c
\end{aligned} \tag{52}$$

$$\begin{aligned}
I_{ac} &= ⨍_{S_{m1}} \frac{1}{r^3}\left[c_{44}^2 D_0 v_0^2(2\delta_{\alpha\beta} - 3r_{,\alpha}r_{,\beta}) + k_{11}(\delta_{\alpha\beta} - 3r_{,\alpha}r_{,\beta})\right]\sqrt{\frac{r}{R}S_c}L_c \mathrm{d}\xi_1\,\mathrm{d}\xi_2 \\
&= 4\Delta\int_0^1 \frac{1}{R^3(\theta)}\left[c_{44}^2 D_0 v_0^2(2\delta_{\alpha\beta} - 3R_{,\alpha}R_{,\beta}) + k_{11}(\delta_{\alpha\beta} - 3R_{,\alpha}R_{,\beta})\right]S_c^{3/2}\mathrm{d}S_c
\end{aligned} \tag{53}$$

The hypersingular integrals related to (50) can be analogously treated. For the case that the reference point P_n coincides with point c or infinitely tends to point b, the related hypersingular integrals can be analogously treated as above. After computing the integrals over all the elements, Eqs. (37)–(39) can now be solved,

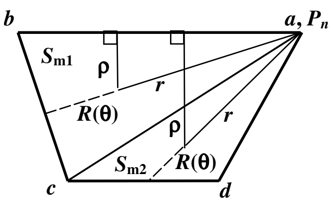

Fig. 2. A crack front element.

and then all the nodal values of $\tilde{u}_i$ and $\tilde{\phi}$ are known, from which the intensity factors at point Q_0 on the crack front can be calculated as follows:

$$K_{\mathrm{I}}(Q_0) = \pi \lim_{Q\to Q_0} [k_{33}\tilde{u}_3(Q) + k_{34}\tilde{\phi}] \cdot (2/\rho)^{1/2} \tag{54}$$

$$K_{IV}(Q_0) = \pi \lim_{Q\to Q_0} [k_{43}\tilde{u}_3(Q) + k_{44}\tilde{\phi}] \cdot (2/\rho)^{1/2} \tag{55}$$

$$K_{\mathrm{II}}(Q_0) = -\pi k_{11} \lim_{Q\to Q_0} \tilde{u}_n(Q) \cdot (2/\rho)^{1/2} \tag{56}$$

$$K_{\mathrm{III}}(Q_0) = \pi c_{44}^2 D_0 v_0^2 \lim_{Q\to Q_0} \tilde{u}_\tau(Q) \cdot (2/\rho)^{1/2} \tag{57}$$

where $(3,n,\tau)$ are the local coordinates.

6. Comparison with elastic isotropic materials

Compared Eqs. (33) and (34) with that for the crack problems in elastic isotropic materials (Qin and Tang, 1993), it can be found that if the term $[k_{33}\tilde{u}_3(Q) + k_{34}\tilde{\phi}(Q)]$ in Eqs. (33) and (54) is replaced with $E\tilde{u}_3(Q)/8\pi(1-v^2)$, Eqs. (33) and (54) will be changed as following

$$\frac{E}{8\pi(1-v^2)} = \!\!\!\!\!\!\neq\!\!\!\!\int_{S^+} \frac{1}{r^3}\tilde{u}_3(Q)ds(Q) = -p_3(P) \quad P \in S^+ \tag{59}$$

$$K_{\mathrm{I}}(Q_0) = \frac{E}{8(1-v^2)} \lim_{Q\to Q_0} \tilde{u}_3(Q) \cdot (2/\rho)^{1/2} \tag{60}$$

Eq. (59) is the same as that for a planar crack in an elastic isotropic material under normal load (Qin and Tang, 1993), and the stress intensity factor (60) will be converted into that for elastic isotropic materials. Similarly, if the term $[k_{43}\tilde{u}_3(Q) + k_{44}\tilde{\phi}]$ in Eqs. (34) and (55) is replaced as $E\tilde{u}_3(Q)/8\pi\,(1-v^2)$, and the electric load q_0 is instead of the elastic load p_3, the electric displacement intensity factor K_{IV} will be equivalent to the stress intensity factor K_{I} (60) for elastic isotropic materials. For mixed mode problems, let that

$$v = 1 + \frac{c_{44}^2 D_0 v_0^2}{k_{11}}, \quad E = -8(1-v^2)k_{11} \tag{61}$$

Then, Eq. (33) is turned to

$$\frac{E}{8\pi(1-v^2)} = \!\!\!\!\!\!\neq\!\!\!\!\int_{S^+} \frac{1}{r^3}[(1-2v)\delta_{\alpha\beta} + 3vr_{,\alpha}r_{,\beta}]\tilde{u}_\beta(Q)ds(Q) = -p_\alpha(P) \qquad \alpha,\beta = 1,2; \quad P \in S^+ \tag{58}$$

which is the same as that for elastic isotropic materials under shear loads. The formula to evaluate the mixed mode stress intensity factors (56) and (57) can be replaced as

$$K_{\mathrm{II}}(Q_0) = \frac{E}{8\pi(1-v^2)} \lim_{Q\to Q_0} \tilde{u}_n(Q) \cdot (2/\rho)^{1/2} \tag{62}$$

$$K_{\mathrm{III}}(Q_0) = \frac{E}{8(1+v)} \lim_{Q\to Q_0} \tilde{u}_\tau(Q) \cdot (2/\rho)^{1/2} \tag{63}$$

Formulae Eqs. (62) and (63) are the same as those for elastic isotropic materials (Qin and Tang, 1993). Therefore, it can be seen that the intensity factors for piezoelectric materials can be obtained from those for elastic isotropic materials.

7. Numerical results

In order to verify above method and illustrate its application, numerical calculations are performed for a crack embedded in an infinite transversely isotropic piezoelectric solid. The piezoelectric materials **PZT-**4 and **PZT-6B** are used for the computations.

7.1. Rectangular crack embedded in an infinite body under normal mechanical loads

Consider a rectangular crack embedded in an infinite transversely isotropic piezoelectric body as shown in Fig. 3. The solid is subjected to normal mechanical load σ_{33}^{∞} and electrical load D_3^{∞} in infinite. In demonstrating the numerical results, the following dimensionless intensity factors will be used

$$F_I = K_I/\sigma_{33}^{\infty}\sqrt{b} \quad F_{IV} = K_{IV}/D_3^{\infty}\sqrt{b} \tag{64}$$

In case of $a/b = 1$, the number of the total nodes is taken as 19×19. Dimensionless stress and electric displacement intensity factors are listed in Table 1, and compared with those given by Chen (2003). It is shown that the present results are satisfied. For general cases, the dimensionless stress and electric displacement intensity factors along the crack front $x_2 = \pm b$ are shown in Fig. 4 for different ratios of a/b. It can be noticed that the stress intensity factors F_I is only related to the mechanical load σ_{33}^{∞}, and the electric displacement intensity factor F_{IV} is related to the electrical load D_3^{∞}.

7.2. Elliptical crack embedded in an infinite body

Let us consider an elliptical crack embedded in an infinite transversely isotropic piezoelectric solid as shown in Fig. 5. The solid is subjected to normal mechanical load σ_{33}^{∞} and electrical load D_3^{∞} in infinite. In

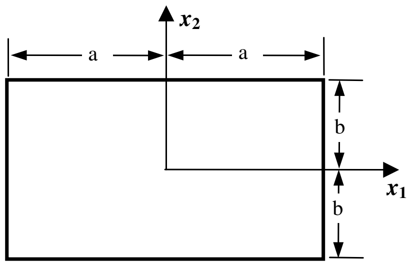

Fig. 3. A rectangular crack.

Table 1
Dimensionless intensity factors F_I,F_{IV}($a/b = 1$)

x_1/a	0	0.143	0.286	0.429	0.571	0.714
Present	0.7533	0.7488	0.7349	0.7095	0.6684	0.6031
Chen	0.7534	0.7488	0.7341	0.7076	0.6645	0.5960

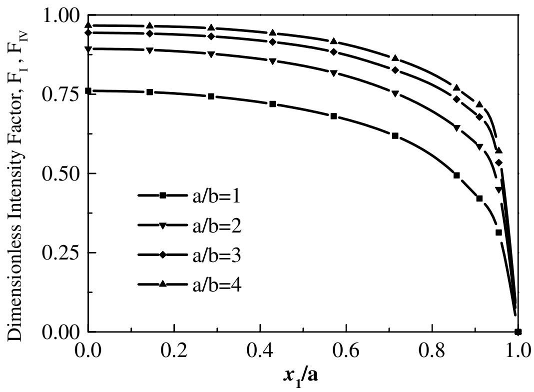

Fig. 4. Dimensionless intensity factors F_I,F_{IV} along the crack front $x_2 = \pm b$.

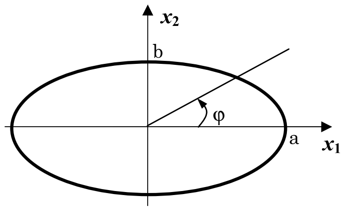

Fig. 5. An elliptical crack.

demonstrating the numerical results, the dimensionless intensity factors are the same as (64). In case of uniform mechanical load and electrical load, the exact solutions of the stress and electric displacement intensity factors have been obtained by Wang and Huang (1995) as follows:

$$F_I = F_{IV} = \frac{(1 - k^2 \cos^2 \varphi)^{1/4}}{E(k)} \tag{65}$$

where $E(k)$ is the complete elliptical integral of the second kind with argument $k^2 = 1 - (b/a)^2$. For different values of ratio a/b, Table 2 gives the maximal dimensionless stress and electric displacement intensity factors F_I, F_{IV} $(x_2 = b)$. In case of $a/b = 2$, Table 3 gives the dimensionless stress and electric displacement intensity factors F_I, F_{IV} along the crack front. It is observed that present results are closed to the exact solutions given by Wang and Huang (1995). For general cases, the dimensionless stress and electric displacement intensity factors along the crack front are shown in Fig. 6 for different ratios of a/b.

Table 2
The maximal dimensionless intensity factor F_I, F_{IV} $(x_2 = b)$

a/b	1	4/3	3/2	2
Present	0.6366	0.7230	0.7536	0.8297
Exact	0.6366	0.7239	0.7564	0.8267

Table 3
The dimensionless intensity factor F_I, F_{IV} $(a/b = 2)$

φ(degree)	0	15	30	45	60	75	90
Present	0.5774	0.5975	0.6569	0.7198	0.7828	0.8253	0.8297
Exact	0.5839	0.6112	0.6716	0.7342	0.7839	0.8151	0.8257
Chen	0.5787	–	–	0.7277	–	–	0.8184
Shang	0.5827	–	–	0.7445	–	–	0.8356

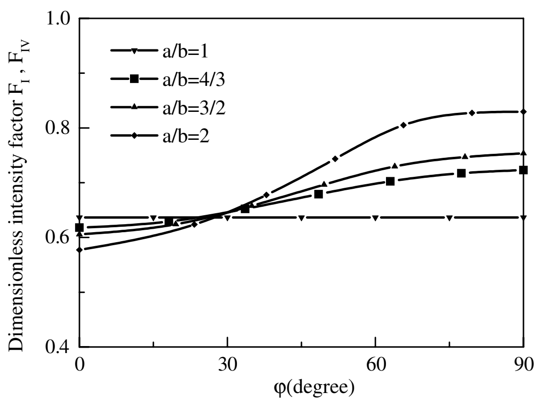

Fig. 6. Dimensionless intensity factors F_I, F_{IV} along the crack front.

8. Conclusion

A flat crack embedded in a three-dimensional infinite transversely isotropic piezoelectric solid subjected to mechanical and electrical loads is analyzed by the finite-part integral method and boundary element method.

1) A set of hypersingular integral equations of an impermeable crack in a three-dimensional infinite transversely isotropic piezoelectric solid subjected to mechanical and electrical loads is derived. It can be observed that crack mode II and mode III are coupled, but independent with mode I and electric mode.
2) Based on the analytical solutions of the singular stresses and electrical displacements near the crack front, a numerical method is proposed by the finite-part integral method and boundary element method, where the square root models of the displacement and electric potential discontinuities in the elements near the crack front are applied. The numerical solutions of the stress and electric field intensity factors of some examples are given. The numerical results show that this numerical technique is successful, and the solution precision is satisfied.
3) From the numerical solutions, it is shown that for an impermeable crack, the mechanical loads will generate the stress intensity factors, and the electric load will generate the "electric field intensity factor" K_{IV}. Moreover, the dimensionless intensity factors of K_I and K_{IV} are independent of the material constants
4) It is shown that the numerical values of the dimensionless intensity factors of K_I and K_{IV} are equal to that of the dimensionless stress intensity factor of mode I for elastic isotropic materials. So, in the case of impermeable cracks, the solutions of intensity factors K_I and K_{IV} can be obtained from the stress intensity factor K_I for elastic isotropic materials.

Acknowledgements

Financial supports from the Science Foundation of Ministry of Education of PR China for the Returned Personnel Studied Abroad is gratefully acknowledged. The useful comments and suggestions provided by the reviewers are also gratefully acknowledged.

References

Chen, M.C., 2003. Application of finite-part integrals to three-dimensional fracture problems for piezoelectric media Part II: numerical analysis. International Journal of Fracture 121, 149–161.
Chen, T., Lin, F.Z., 1995. Boundary integral formulations for three-dimensional anisotropic piezoelectric solids. Computational Mechanics 15, 485–496.
Daros, C.H., Antes, H., 2000. Dynamic fundamental solutions for transversely isotropic piezoelectric materials of crystal class 6 mm. International Journal of Solids and Structures 37 (11), 1639–1658.
Deeg, W.F.J., 1980. The analysis of dislocation, crack, and inclusion problems in piezo-electric solids. PhD thesis. Stanford University.
Dunn, M.L., Wienecke, H.A., 1996. Green's functions for transversely isotropic piezo-electric solids. International Journal of Solids and Structures 33 (30), 4571–4781.
Hill, L.R., Farris, T.N., 1998. Three-dimensional piezoelectric boundary element method. AIAA Journal 36 (1), 102–108.
Khutoryansky, N., Sosa, H., 1995. Dynamic representation formulas and fundamental solutions for piezoelectricity. International Journal of Solids and Structures 32 (22), 3307–3325.
Kumar, S., Singh, R.N., 1996. Crack propagation in piezoelectric materials under combined mechanical and electrical loadings. Acta Materilia 44, 173–200.
Liu, Y.J., Fan, H., 2001. On the conventional boundary integral equation formulation for piezoelectric solids with defects or of thin shapes. Engineering Analysis with Boundary Elements 25, 77–91.
McMeeking, R.M., 1999. Crack tip energy release rate for a piezoelectric compact tension specimen. Engineering Fracture Mechanics 64, 217–244.
Norris, A.N., 1994. Dynamic Green's functions in anisotropic piezoelectric, thermoelastic and poroelastic solids. Proceedings of the Royal Society of London, Series A 447, 175–188.
Pak, Y.E., 1990. Crack extension force for a piezoelectric material. ASME Journal Applied Mechanics 57, 647–653.
Park, S., Sun, C.T., 1995. Fracture criteria for piezoelectric ceramics. Journal of the American Ceramic Society 78, 1475–1480.
Qin, Q.H., 2001. Fracture mechanics of piezoelectric materials. WIT Press, Southampton, Boston.

Qin, T.Y., Noda, A.K., 2004. Application of hypersingular integral equation method to a three-dimensional crack in piezoelectric materials. JSME, International Journal Series A 47 (2), 173–180.
Qin, T.Y., Tang, R.J., 1993. Finite-part integral and boundary element method to solve embedded planar crack problems. International Journal of Fracture 60, 373–381.
Qin, T.Y., Chen, W.J., Tang, R.J., 1997. Three-dimensional crack problem analysis using boundary element method with finite-part integrals. International Journal of Fracture 84 (2), 191–202.
Rajapakse, R.K.N.D., Xu, X.L., 2001. Boundary element modeling of piezoelectric solids. Engineering Analysis with Boundary Elements 25, 771–781.
Shang, F., Kuna, M., Abendroth, M., 2003. Finite element analyses of three-dimensional crack problems in piezoelectric structures. Engineering Fracture Mechanics 70, 143–160.
Suo, Z., Kuo, C.M., et al., 1992. Fracture mechanics for piezoelectric ceramics. Journal of the Mechanics Physics of Solids 40, 739–765.
Wang, B., 1992. Three-dimensional analysis of an elliptical crack in a piezoelectric material. International Journal of Engineering Science 30, 781–791.
Wang, Z.K., Huang, S.H., 1995. Fields near elliptical crack in piezoelectric ceramics. Engineering Fracture Mechanics 51, 447–456.
Wang, B.L., Zhang, X.H., 2005. Fracture prediction for piezoelectric ceramics based on the electric field saturation concept. Mechanics Research Communications 32, 411–419.
Zhao, M.H., Shen, Y.P., et al., 1997. Isolated crack in three-dimensional piezoelectric solid. Part II: stress intensity factors for circular crack. Theoretical and Applied Fracture Mechanics 26, 141–149.